Ann. Geophys., 31, 61–73, 2013
www.ann-geophys.net/31/61/2013/
doi:10.5194/angeo-31-61-2013

Annales Geophysicae

Development of the mesospheric Na layer at 69° N during the Geminids meteor shower 2010

T. Dunker[1], **U.-P. Hoppe**[2,1,*], **G. Stober**[3], **and M. Rapp**[3,**]

[1]University of Tromsø, Department of Physics and Technology, 9037 Tromsø, Norway
[2]University of Oslo, Department of Physics, P.O. Box 1048 Blindern, 0316 Oslo, Norway
[3]Leibniz-Institute of Atmospheric Physics (IAP), Schlossstraße 6, 18225 Ostseebad Kühlungsborn, Germany
[*]on leave from: Norwegian Defence Research Establishment (FFI), P.O. Box 25, 2027 Kjeller, Norway
[**]now at: German Aerospace Center (DLR), Institute of Atmospheric Physics (IPA), Münchner Straße 20, 82234 Oberpfaffenhofen-Wessling, Germany

Correspondence to: T. Dunker (tim.dunker@fys.uio.no)

Received: 15 August 2012 – Revised: 22 November 2012 – Accepted: 5 December 2012 – Published: 9 January 2013

Abstract. The ECOMA sounding rocket campaign in 2010 was performed to investigate the charge state and number density of meteoric smoke particles during the Geminids meteor shower in December 2010. The ALOMAR Na lidar contributed to the campaign with measurements of sodium number density, temperature and line-of-sight wind between 80 and 110 km altitude over Andøya in northern Norway. This paper investigates a possible connection between the Geminids meteor shower and the mesospheric sodium layer. We compare with data from a meteor radar and from a rocket-borne in situ particle instrument on three days. Our main result is that the sodium column density is smaller during the Geminids meteor shower than the winter average at the same latitude. Moreover, during two of the three years considered, the sodium column density decreased steadily during these three weeks of the year. Both the observed decrease of Na column density by 30 % and of meteoric smoke particle column density correlate well with a corresponding decrease of sporadic meteor echoes. We found no correlation between Geminids meteor flux rates and sodium column density, nor between sporadic meteors and Na column density ($R = 0.25$). In general, we found the Na column density to be at very low values for winter, between 1.8 and $2.6 \times 10^{13}\,\mathrm{m}^{-2}$. We detected two meteor trails containing sodium, on 13 December 2010 at 87.1 km and on 19 December 2010 at 84 km. From these meteor trails, we estimate a global meteoric Na flux of $121\,\mathrm{kg\,d}^{-1}$ and a global total meteoric influx of $20.2\,\mathrm{t\,d}^{-1}$.

Keywords. Atmospheric composition and structure (Middle atmosphere – composition and chemistry; Instruments and techniques; General or miscellaneous)

1 Introduction

One might expect the Geminids to increase the density or modify other characteristics of the sodium layer, at least during the time of their peak activity. The purpose of this work is to investigate if the influx of meteoric material during the Geminids meteor shower has any significant influence on the mesospheric sodium layer at high latitudes. The Geminids in 2010 had their peak activity in the night from 13 to 14 December. Our data set covers almost 40 h of lidar measurements on six days in 2010 – before, at the peak and shortly after the Geminids shower activity. Furthermore, we compare similar data from 2009 and 2011, as well as meteor radar data from December 2010 and in situ particle measurements from December 2010.

It has been known since 1929 that emissions in the atmosphere near the sodium (Na) resonance line exist (Slipher, 1929). It is well-known that meteors are the source of mesospheric metal species like sodium, potassium and iron, which exist in their atomic state in a layer between about 80 to 110 km altitude (Junge et al., 1962). The first lidar observation of atmospheric Na was reported by Bowman et al. (1969), and numerous studies have since been carried out

to investigate the mesospheric metal layers at different latitudes.

The mesospheric Na layer exhibits a seasonal variation. In the summer months (June, July, August), Na density is smallest, while it is greatest during the winter months (November, December, January). The Na density decreases and increases gradually during spring and autumn (e.g. Plane et al., 1999). Their study was performed for mid-latitude conditions, but the same annual pattern is visible at high latitudes. Tilgner and von Zahn (1988) measured during the 1985/86 winter at Andøya. They found an average Na column density of $5.6 \times 10^{13}\,\mathrm{m}^{-2}$ and no obvious trend for that winter season.

Chemistry plays a key role in the abundance of mesospheric Na (see Plane, 2003, for a review of metal chemistry in the atmosphere). The major reservoir for Na below 90 km is believed to be the molecule $NaHCO_3$, which has a relatively long lifetime in the mesosphere (Plane, 2000). Above 95 km, Na^+ is the major reservoir species for atomic Na (Helmer and Plane, 1993). Another sink is the uptake of $NaHCO_3$ and Na^+ on meteoric smoke particles, likely highly efficient, where Na species adsorb on silica (SiO_2) surfaces (Plane, 2004). Models for the mesospheric Na layer have been developed by Helmer and Plane (1993) and McNeil et al. (1995). Their results indicate that more than 90 % of the total Na at 95 km occurs as atomic Na.

There are only a few studies that have investigated the abundance of Na^+ in the mesosphere and lower thermosphere. Kopp (1997) published the results of five sounding rocket launches, one of them on 30 November 1980 at Kiruna, Sweden (67.9° N, 21.1° E), which is located east of the Scandinavian mountain range, almost at the same latitude as the Andøya Rocket Range. Kopp (1997) calculated a Na^+ column density of $1.9 \times 10^{12}\,\mathrm{m}^{-2}$ for four of the rocket flights and found that the ion abundance during the launch close to the Geminids was not different from periods without meteor shower activity.

The Geminids are a major meteor shower with a zenithal hourly rate of 120 meteors (Correira et al., 2010), making the Geminids (together with the Quadrantids) the most pronounced of all meteor showers. Meteor shower activity starts around 9 December, peaks at 13/14 December and decays rapidly thereafter, with the last activity around 16 December. The Geminids can be well distinguished from sporadic meteors by their radiant, the apparent direction of their origin in astronomical coordinates. The peak meteor flux occurs at a solar longitude of 262°. Between 40 % and 50 % of all observed radar meteors originate from the Geminids radiant during peak activity (Stober et al., 2012).

Borovička (2006a) reported a significant Na depletion for most of the Geminids, among other meteor showers. However, depletion is not complete, and the amount of Na varies from meteoroid to meteoroid (Borovička, 2006a), with the level of depletion being a measure for the meteoroid's age. A spectroscopic analysis revealed that the level of Na depletion is stronger in the meteors occurring before the maximum (Borovička, 2006b). The Na abundance by mass is 0.6 % (Mason, 1971) under the assumption that most meteoric material has the composition of ordinary chondrites.

Rietmeijer (2003) mentions a scenario where influx of high-velocity comet meteoroids and low-velocity near-Earth asteroids could be the cause for seasonal variations in mesospheric sodium, potassium and carbon abundance. The Geminids have a high entry velocity of about $36\,\mathrm{km\,s}^{-1}$ (Stober et al., 2012). They are of cometary origin (Borovička, 2006a), but their parent body is the near-Earth asteroid 3200 Phaethon. This obvious contradiction is underscored by the comet-like orbit of 3200 Phaeton and the fact that its surface is very dark and that it never develops a cometary tail.

Hughes (1978) estimated the global annual mass influx from the Geminids as 15 t, the influx from the Perseids and Quadrantids as only 2.6 t each. The Geminids are also the meteor stream with the greatest density ($1.06 \times 10^3\,\mathrm{kg\,m}^{-3}$), about three times greater than the density of sporadic meteors and all the other known meteor showers (Hughes, 1978). Modern meteor smoke simulations, for instance Kalashnikova et al. (2000), typically assume a particle bulk density of $2.5 \times 10^3\,\mathrm{kg\,m}^{-3}$, but for meteors in general, not for the Geminids. In this paper, we use neither of these values, but merely report the scatter of values we have found in the literature. A much greater mass influx for the Geminids of 35 t distributed over ten days of activity is reported by Correira et al. (2010), but the mass influx is not equally distributed over those ten days. Almost all material is ablated between 12 and 14 December (Stober et al., 2012), yielding a greater mass influx during the peak activity than the average of $3.5\,\mathrm{t\,d}^{-1}$ given by Correira et al. (2010).

An influence by meteor showers on the neutral metal layers has long been suspected. Yet, evidence has not always been found. There have been some studies investigating a possible correlation between neutral metal densities and the influx of meteor material during meteor showers. Some of the authors report an influence (Uchiumi et al., 1993; Gerding et al., 1999; Höffner et al., 1999), but mostly for a very short time. From four hours of lidar measurements, a fourfold increase in Na density was reported by Hake et al. (1972). No influence has been found by Höffner et al. (2000) and Chu et al. (2000). Concerning the metal layer topside, above 110 km altitude, Höffner and Friedman (2004) found evidence for a connection between meteoric influx and the potassium and calcium densities at Kühlungsborn, Germany, and Arecibo, Puerto Rico. Correira et al. (2010) used GOME satellite data to study the magnesium atom (Mg) and ion (Mg^+) column density in the atmosphere for the period 1996 to 2001. They have not found an increase in column density for these species during meteor shower activity.

Clemesha et al. (1978) first reported on the occurrence of sporadic Na layers. These authors have proposed that direct meteor input might cause these sporadic Na layers. Later, Clemesha (1995) and Clemesha et al. (1999) did not rule out direct meteor input, but stated that evidence for a correlation

between occurrence of sporadic Na layers and meteor showers was not conclusive. Cox and Plane (1998) suggested an ion-molecule formation mechanism for sporadic Na layers, that was tested experimentally by Heinselman et al. (1998) and Heinselman (2000). Clemesha et al. (1999) concluded the ion-recombination mechanism to be the most likely cause for sporadic Na layers. Other studies of sporadic Na layers by lidar at high latitudes have suggested mechanisms for their generation unrelated to direct meteor input: von Zahn et al. (1987), von Zahn and Hansen (1988), Hansen and von Zahn (1990), Heinselman et al. (1998), Nesse et al. (2008), Heinrich et al. (2008).

We will first describe our instruments, briefly investigate the atmospheric conditions during the lidar measurements and then concentrate on the Na layer properties and their relation to meteor flux rates and meteoric smoke particles.

2 Instruments

We have measured with the ALOMAR Weber Na lidar and the Andenes SKiYMET meteor radar, on the Norwegian island Andøya, on several days in the period from 26 November until 19 December 2010, covering the time of the Geminids meteor shower. These lidar and radar measurements were part of the ECOMA programme, a German–Norwegian sounding rocket project with a last campaign in December 2010 at the Andøya Rocket Range. The acronym ECOMA stands for "Existence and Charge state Of meteoric smoke particles in the Middle Atmosphere". During the campaign, the rockets ECOMA 7, 8 and 9 were launched. All three rockets were launched under similar conditions, when there was a quiet ionosphere and no auroral particle precipitation. The ground-based instruments covered the rocket launches on 13 and 19 December. The atmospheric volumes that were probed by rocket and lidar were separated horizontally by approximately 20 to 40 km.

2.1 ALOMAR Weber Na lidar

The Na lidar at ALOMAR (Arctic Lidar Observatory for Middle Atmosphere Research) is a narrowband resonance fluorescence lidar located at 379 m above mean sea level on top of Ramnan mountain (69.3° N, 16.0° E), about 2 km south-southwest of the Andøya Rocket Range, on the northern Norwegian island of Andøya. She et al. (2002), Arnold and She (2003) and Kaifler (2009) have described this Na lidar in detail. It is owned and operated by GATS, Inc., the University of Tromsø and the Andøya Rocket Range. Former co-owners were Colorado State University and Colorado Research Associates, whose expertise has been transferred to GATS, and FFI.

The Na lidar measures Na number density, line-of-sight wind speed and temperature in the altitude range between about 80 and 110 km with uncertainties better than $10^8\,\mathrm{m}^{-3}$, $2\,\mathrm{m\,s}^{-1}$ and 2 K, respectively. Mesospheric temperature measurements using the Na D_2 resonance line were first reported by Gibson et al. (1979) and by Thomas and Bhattacharyya (1980). The measurement principle is based on probing the Doppler broadening and Doppler shift of the Na resonance line D_{2a}, a method described by Fricke and von Zahn (1985). The altitude range depends on season, because the extent of the Na layer exhibits a seasonal variation with the largest extent in winter. The lidar measures atomic Na, but no molecular or ion species.

The Na Weber Lidar operates at 50 Hz and emits laser pulses with a wavelength of 589 nm and a duration of 6.7 ns FWHM (full width at half maximum). A cycle of three frequencies is emitted by the lidar, one at the D_{2a} frequency of Na (589.189 nm) and the other two at $+630$ ($\pm$ 50) and -630 ($\pm$ 50) MHz relative to the D_{2a} frequency.

At first, continuous-wave (cw) 589 nm light with a power of up to 70 mW is created through sum-frequency generation of two cw Nd:YAG beams at 1319 nm and 1064 nm. This 589 nm beam is locked to the Lamb dip at the Na D_{2a} resonance line (589.189 nm) using Doppler-free spectroscopy. An acousto-optic modulator generates two additional frequencies at $\pm$630 MHz, relative to the D_{2a} line. These three frequencies are emitted in cycles with lengths of 15 s, such that each frequency is emitted for five seconds. This cw light enters a Spectra Physics Quanta-Ray Pulsed Dye Amplifier 1, consisting of three dye cells, i.e. amplification stages. The dye amplifier is pumped by a pulsed, frequency-doubled Spectra-Physics Quanta-Ray PRO 230 Nd:YAG operating at 50 Hz, yielding the pulsed 589 nm beam. The spectral FWHM of the lidar pulses is 130 MHz, corresponding to 0.15 pm. The output beam is guided through a beam expander, such that the beam diameter is widened to 20 mm and the divergence is reduced to 450 µrad. A beamsplitter divides the beam into two branches of equal power. Beamsteering mirrors guide the beams to the atmosphere and move each beam such that there is a full overlap with the lidar field of view at the Na layer altitudes. The lidar field of view is 600 µrad (full angle). Due to the laser divergence, the instrument probes an atmospheric volume with a diameter of 45 m at 100 km altitude.

The photons emitted by the laser are scattered by the mesospheric Na atoms, and the backscattered photons are collected with two telescopes ($ø = 1.8$ m). The telescopes belong to the RMR lidar, owned and operated by the Leibniz-Institute of Atmospheric Physics in Kühlungsborn, Germany (von Zahn et al., 2000). They can be pointed to zenith angles between 0° and 30° and azimuth angles between 270° to 360° and 90° to 180°, respectively. Fibres guide the photons to a mechanical chopper that operates at 50 Hz, cutting off parts of the tropospheric signal. After the chopper, the photons pass an interference filter with a bandpass of 1 nm, centered at 589 nm. Finally, the photons are counted with photomultiplier tubes (Hamamatsu R932-02) and stored to disk with an altitude bin size of 150 m.

Table 1. Beam specifications for the ALOMAR Na lidar, including lidar field of view (as of 21 December 2010). For the 589 nm laser beam, only data for the D_{2a} frequency is given. Beam divergence is given as full angle. Pulse length is given as full width at half maximum (FWHM).

Beam spec.	Pulsed 589 nm
Power [W]	1
Rep. rate [Hz]	50
Pulse energy [mJ]	20
Pulse length [ns]	6.7
Beam diameter [mm]	20
Beam div. [µrad]	450

Table 2. Rocket launches and lidar observations during the ECOMA campaign 2010. Only days with more than three hours of data are listed. Times are given in [hh:mm] format in UT. Local time is UT plus one hour.

Day	Rocket launch	Na lidar observation
26 November	–	16:38–23:12
4 December	04:21 (ECOMA 7)	19:32–23:07
5 December	–	18:37–22:37
7 December	–	13:25–18:35
13 December	03:24 (ECOMA 8)	02:40–07:20
19 December	02:36 (ECOMA 9)	01:34–08:48
		13:14–21:52
Sum [hh:mm]		39:51

The geophysical variables can be calculated from the recorded photon count profiles at the three frequencies, but some necessary corrections have to be applied to the data (Heinrich, 2007; Heinrich et al., 2008). The background has to be subtracted from the data, we have to correct for the deadtime of the photomultipliers and for the different pulsed output power at the three frequencies, also over time. The photon count profiles at the altitudes of the Na layer are normalized to the photon counts from the stratosphere at 38 km, which we assume as aerosol-free. In that case, all counts are purely due to Rayleigh scattering. The emitted frequencies are so similar that the Rayleigh scattering coefficient is assumed to be the same. Hence, the photon counts depend only on output power, but not on frequency, and can be normalized to each other. Above the normalization altitude, we consider the atmospheric transmission to be unity, but we correct for differential extinction in the Na layer. We obtain the atmospheric density at the normalization altitude from ECMWF reanalysis data, issued every six hours for Andenes. The Na number densities can then be measured directly (Fricke and von Zahn, 1985). Doppler broadening and Doppler shift of the Na D_{2a} resonance line are used to measure temperature and line-of-sight winds (Fricke and von Zahn, 1985; Arnold and She, 2003).

The amount of Na atoms in an atmospheric column is given by the column density C:

$$C = \int_{z_0}^{z_\mathrm{H}} n(z)\,\mathrm{d}z. \quad (1)$$

In Eq. (1), z_0 and z_H denote the bottom and the top altitude of the Na layer, respectively, with the Na number density $n(z)$ at the corresponding altitude z. The centroid height z_c of the Na layer can be calculated using Eq. (2). This parameter is rather insensitive to wave perturbations and therefore a good indicator of the Na layer state (Gardner et al., 1986).

$$z_c = \frac{\int_{z_0}^{z_\mathrm{H}} n(z)\cdot z\,\mathrm{d}z}{\int_{z_0}^{z_\mathrm{H}} n(z)\,\mathrm{d}z} \quad (2)$$

Assuming a Gaussian profile for each of the recorded Na density profiles, the FWHM of the Na layer can be calculated, which is related to the RMS width (Gardner et al., 1986).

Lidar specifications during the ECOMA campaign 2010 are given in Table 1. During the campaign, we operated the Na lidar between 26 November 2010 and 19 December 2010, whenever there was clear sky. The operational dates and times are listed in Table 2.

For this study, we use a running mean of ten altitude bins, yielding a height resolution of 1.5 km. The temporal resolution is five minutes, unless otherwise noted. The data presented here was taken with the two telescopes always pointed to north and east, respectively, with a zenith angle of 20° each. This was done in order to measure the meridional and zonal wind components. We concentrate on the data from the northward pointing beam because the uncertainties are slightly better compared to the eastward beam. Both beams show essentially the same time development of the Na layer.

The exception is the Na column density data from 2011, when the telescopes pointed to zenith.

2.2 Andenes meteor radar

The Leibniz-Institute of Atmospheric Physics at Kühlungsborn operates a standard all-sky SKiYMET meteor radar at Andenes. The system is located approximately 1.5 km east of the ALOMAR observatory. The radar operates at a frequency of 32.55 MHz and transmits a peak power of 30 kW. The antenna array consists of five receiving and one transmitting antenna. The radiation pattern is almost symmetrical due to the use of crossed dipole antennae (Singer et al., 2004). A more detailed description of the experiment configuration is given by Stober et al. (2012).

The specular meteor observations are suitable to investigate the astrophysical properties of the meteoroids, like the source radiant (on a statistical basis), entry velocity, altitude, meteor count rate and the ablation rate (electron line density). The radar is also capable of measuring atmospheric winds in the altitude range between 78 and 100 km.

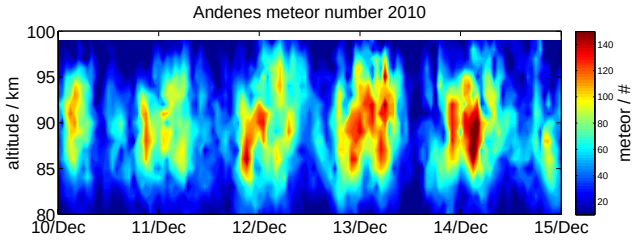

Fig. 1. Time series of total meteor counts per altitude for the period 10 to 14 December 2010, measured with the Andenes SKiYMET meteor radar. Peak activity on the night from 13 to 14 December, with almost equal activity on the night before. Note the strong decrease in total meteor counts in the night from 14 to 15 December.

2.3 The ECOMA particle detector

Each of the three sounding rockets carried an ECOMA particle detector as described in detail by Rapp and Strelnikova (2009) and Rapp et al. (2010). Briefly, this detector combines a classical Faraday cup design (e.g. Havnes et al., 1996) for the detection of naturally charged heavy particles with an active photo-ionization of mesospheric smoke particles with a Xenon flash lamp and the subsequent detection of corresponding photoelectron pulses. A classical Faraday cup basically consists of a cylindrical metallic bucket which contains the detector electrode at the bottom of the cylindrical structure. This structure is exposed to the ambient air flow by the rocket motion because it is mounted on the payload's top deck and aligned with the rocket axis. The structure is covered with two shielding grids biased at -3 V (outer grid) and $+3$ V (second grid) to prevent positive ions and electrons from entering the detector volume and creating a current at the electrode. Only large and heavy aerosol particles have sufficient energy to pass these potential barriers, reach the electrode, and create a current if they are charged. This method is affected by aerodynamical effects. For instance, too light particles can be deflected by the shock front ahead of the detector and never reach the electrode. Therefore, this type of meteoric smoke particle detection only works above a certain altitude (cut-off ~ 80 km). For the purpose of the current study, we will solely focus on the detection of these naturally charged particles. Further details about the particle detector measurements are presented in the companion paper by Rapp et al. (2012).

3 Results

3.1 SKiYMET Andenes meteor radar

The total meteor fluxes (sporadic and shower meteors) measured with the Andenes SKiYMET meteor radar are shown in Fig. 1. The time resolution is 30 min and the time period ranges from 10 December 2010, 00:00 UT until 14 December 2010, 23:59 UT. We see a gradual increase in total meteor counts until 14 December, when the maximum total meteor count rates are measured. After that, the total meteor count rates decrease rapidly, indicating that the meteor shower is almost over, see also Stober et al. (2012). The maximum total number of meteors occurs each day from around 23:00 UT until approximately 05:00 UT the next day. The peak activity of the Geminids 2010 was reached on 14 December, with maximum total meteor flux rates of 1000 to 1200 meteors per hour, integrated over all altitudes. The maximum total meteor flux rate on 13 December 2010 was slightly lower than on 14 December (about 1000 meteors per hour).

3.2 Sodium layer

We only use measurement data of at least three hours' duration that were taken during darkness. Even though the sun does not rise during late November and in December, the sky becomes too bright to measure without daylight filters at Andenes between about 10:00 and 13:00 UT. We only use data from the beam pointed northward with a zenith angle of 20°. The eastward beam (zenith angle 20°) essentially shows features similar to the northward beam (see also Sect. 2.1). Using this telescope setup, the volumes probed by the lidar beams are separated horizontally by 51 km at an altitude of 100 km. An exception is the data from December 2011, see Fig. 7. On those four days the telescopes were pointed to zenith.

By chance we also observed two meteor trails, confirming the known fact that sporadic meteors contain Na, and probably some Geminids as well. Figure 2a shows a meteor trail at 84 km. It was neither observed during the previous 30 s, nor during the following. This trail must be from a sporadic meteor, several days after the end of the Geminids. Because of its vertical extent, we can assume that it has had several seconds to minutes to diffuse to such a diamete. The lidar observes the trail because it contains atomic Na. The meteor increases the Na number density at 84 km to about $1950 \times 10^6\,\mathrm{m}^{-3}$, an increase by 25 % relative to the background density at that altitude. We do not classify this thin layer as a sporadic Na layer due to the very short time (visible for less than a minute) and the very narrow altitude range.

Figure 2b shows a fresh meteor trail, most likely from a Geminid. Each line shows the 5-s integral of normalized counts for the datafile starting on 13 December 2010 at 03:31:52 UT, lasting for 15 s (i.e. five seconds per frequency). Each colour represents one of the three transmitted lidar frequencies (see figure caption). The Na D_{2a} resonance frequency (red line) is the first emitted frequency of each cycle. We see a steep increase of counts by approximately 60 % near 87 km. In the upshifted frequency (green line), the increase is approximately a factor of five over the Na background at that height, while the intensity has decreased to less than 60 % five seconds later, when the lidar transmitted the downshifted frequency (blue line). Because of the trail's small vertical extent (less than 150 m) and short

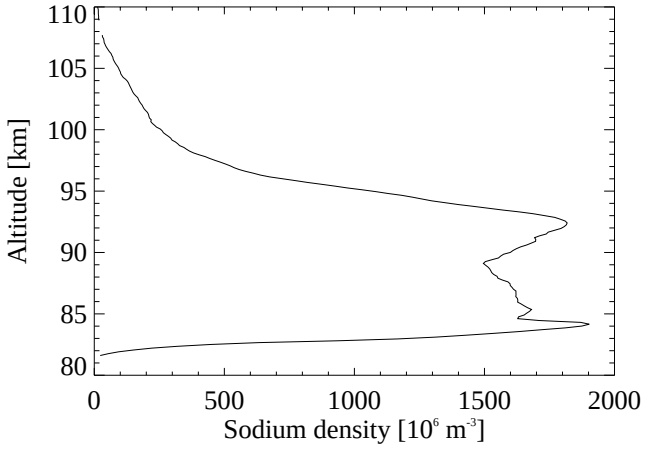

Fig. 2a. Sodium number density on 19 December 2010, 00:38:30 UT. Average of 30 s. Beam pointing: zenith. The sporadic meteor trail at 84 km was observed for less than a minute.

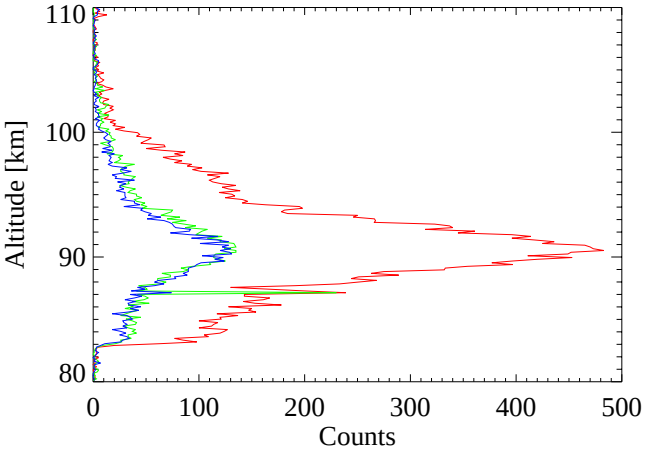

Fig. 2b. Sodium resonance signal (normalized photon counts) on 13 December 2010, 03:31:52 UT. Each colour represents the 5-s integral from one of the lidar frequencies. Solid red line: unshifted D_{2a} frequency; green and blue lines: up- and downshifted frequencies. The Geminid meteor trail at 87 km has a maximum of 240 counts. It is first visible at the D_{2a} frequency (red line). The meteor trail was visible for 15 s in the lidar beam and only in one altitude channel (150 m). See text for details.

duration (small horizontal extent of the trail drifting through the lidar beam), this must be a fresh meteor trail. On this day the meteor radar observed nine times more Geminids than sporadic meteors, therefore the probability that Fig. 2b shows a Geminid trail is about 90 %. Because the duration of the meteor trail signal is shorter than a full lidar measurement cycle of 15 s, we can only estimate the amount of Na deposited by assuming unchanged temperature and line-of-sight wind. It would have been interesting to compare the actual Na temperature inside the meteor trail with the ambient temperature, but the duration was too short. We estimate $3900 \times 10^6\,\mathrm{m}^{-3}$, almost equal to the Na density at peak altitude ($3910 \times 10^6\,\mathrm{m}^{-3}$). Figure 2b does not show Na density in absolute numbers.

Figures 2a and 2b show the only meteors observed with the lidar during 39:51 h of measurements in November and December 2010. From the fact that we did not observe only one meteor, and not three, we can put limits on the amount of sodium ablated at this latitude in December from meteors that are above the detection threshold of this lidar: The mean Na density of both meteor trails is approximately $2.9 \times 10^9\,\mathrm{m}^{-3}$. The Na meteor trail has a vertical extent of about 150 m. From these values, we estimate an Na flux of $2.3 \times 10^{-13}\,\mathrm{kg\,m^{-2}\,d^{-1}}$. Thus, the global Na flux at 85 km is approximately $121\,\mathrm{kg\,d^{-1}}$. The global meteoric input per day is approximately $20.2\,\mathrm{t\,d^{-1}}$ if we assume that 0.6 % of the meteor mass is sodium (Mason, 1971). Plane (2004) reports that the daily global meteoric input has to be smaller than $20\,\mathrm{t\,d^{-1}}$. The detection limit of the Na lidar is a meteoric flux of about $10^{-11}\,\mathrm{kg\,m^{-2}\,s^{-1}}$.

The time series of Na column density for selected days of the ECOMA campaign are shown in Figs. 3 to 5. We concentrate on the days of the rocket launches, i.e. 4, 13 and 19 December 2010. The measurement periods and durations for all days of the campaign are given in Table 2. For comparison, we have also included measurement data from December 2009 and December 2011 in Fig. 7. Measurements were performed at different times of day, but always in darkness. The distribution of our measurements compared to any tidal variation happened to be rather even, so that any tidal variation would change the mean and median values only by a small amount. We see that the Na column density is subject to variation, but according to Granier and Mégie (1982) and Clemesha et al. (1982) the Na layer does not exhibit a significant diurnal variation. Plane (2004) has shown that the lack of a diurnal variation of the Na layer can be caused by the uptake of $NaHCO_3$ (the major Na reservoir species below about 85 km) on meteoric smoke particles. That study was carried out for mid-latitudes.

If the actual atmospheric density at our normalization altitude (see Sect 2.1) deviated from the ECMWF reanalysis that we use by 1 to 2 %, the values and variations of Na column density in Figs. 3 to 5 would contain a systematic error by the same amount. Also, if the the stratosphere at the normalization altitude did contain aerosol contrary to our assumption, we would underestimate the actual Na density.

The first rocket of the 2010 campaign, ECOMA 7, was launched on 4 December at 04:21 UT. Lidar observations were not possible during the launch due to clouds, but began 14 h later, lasting from 18:12 UT until 23:37 UT. Figure 3 shows the time series of Na column density. On 4 December, the Geminids had not yet begun.

The second rocket (ECOMA 8) was launched on 13 December at 03:24 UT, during the peak activity of the Geminids. This rocket launch was covered by lidar observations lasting from 02:40 UT until 07:20 UT. The time series of Na column density is shown in Fig. 4. No rapid and large

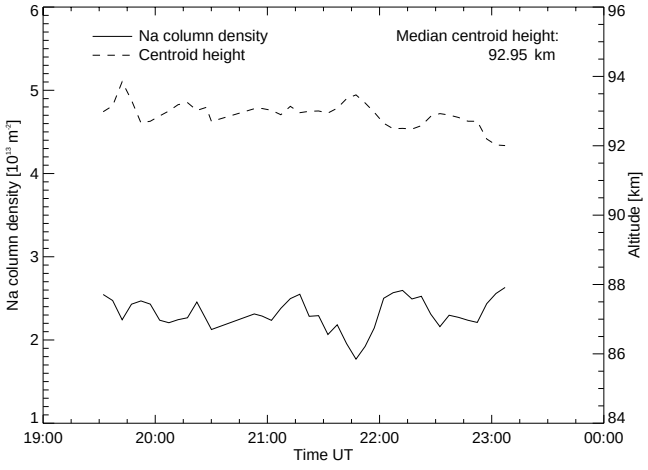

Fig. 3. Time series of Na column density for the northward pointing beam on 4 December 2010. The temporal resolution is five minutes.

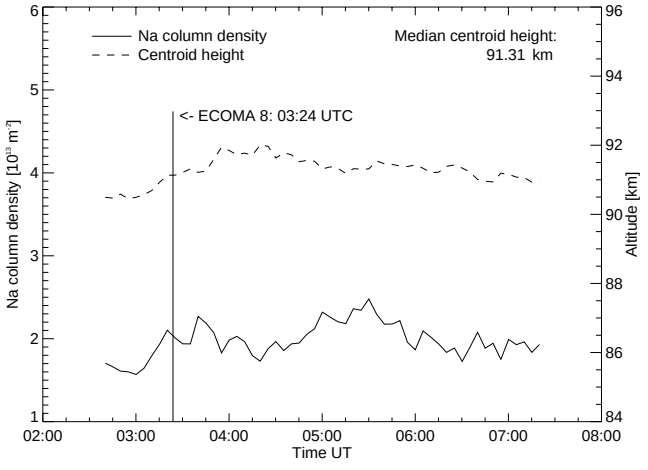

Fig. 4. As Fig. 3, but 13 December 2010. The vertical line indicates the launch of ECOMA 8.

increase in Na column density is visible, even though the column density varies over time. The total meteor count rates are shown in Fig. 1. The FWHM of the Na layer is very narrow on 13 December, only 7.82 km, but the peak density is greater than on the other days (see Table 3). The bottom of the Na layer is, as usual, at about 80 km altitude, and the layer becomes undetectable above only 103 km. Despite the meteor shower, we did not observe an increased topside abundance (Höffner and Friedman, 2004) or sporadic Na layers as suggested by Clemesha et al. (1978).

Figure 5 shows the time series of Na column density on 19 December 2010, when the third and final rocket ECOMA 9 was launched (02:36 UT). We performed Na lidar observations from 00:18 until 08:48 UT and again from 13:14 until 21:52 UT. The centroid height of the Na layer is 90.97 km, the lowest value measured during the campaign, but the FWHM increased to 10.64 km. The median column density is $1.81 \times 10^{13}\,\mathrm{m}^{-2}$, also the smallest value of the campaign. On 19 December, the Geminids meteor shower was already over (Stober et al., 2012). Thus, the variations of Na column density on this day cannot be due to the meteor shower.

The ALOMAR Weber Na lidar was also used to measure the temperature at the Na layer altitudes (Fig. 6 and Table 3). In the following, we discuss mean values for each night's lidar observations. At 91 km, approximately at the altitude of the Na peak density, the temperature rises from 201 K (26 November) to 207 K (4 December), and decreases to 199 K on 5 December. The minimum value is reached on 7 December with 198 K. On 13 December, the temperature has risen to almost 222 K. These temperatures measured by the Na lidar are consistent with temperatures measured with the Andenes meteor radar (not shown here). Throughout December, the temperatures appear to be normal for the winter season (Lübken and von Zahn, 1991; Neuber et al., 1988), with the exception of 13 December. The temperature generally decreases with increasing altitude throughout December 2010, but this changes on 13 December, when temperatures increases at 85, 91 and 97 km and a mesospheric inversion layer is observed (see Szewczyk et al., 2012, for the study of a mesospheric inversion layer on 19 December 2010). On 13 December, the Na lidar measured the highest temperatures between 90 and 95 km.

On time scales of days, sodium density and temperature are positively correlated through chemistry, but the correlation is not entirely linear (Plane et al., 1998). On time scales of gravity waves (minutes to hours), Na density and temperature vary due to dynamics. Tilgner and von Zahn (1988) reported an average Na column density of $5.6 \times 10^{13}\,\mathrm{m}^{-2}$ for the winter season 1985/86, with no significant seasonal trend. For the same winter, Neuber et al. (1988) reported mean temperatures of 200 to 205 K for the region between 90 and 95 km.

If a higher temperature always led to an increase of Na, we should have seen a larger abundance on 13 December 2010 than on the other days of the campaign. This is not the case. The peak density is, however, greater on 13 December than on the other days, but this has no effect on the column density. Because the measured temperatures are not unusual for December, the generally low and decreasing values of Na column density cannot be explained by temperature alone.

We have computed the median Na column density and uncertainty for each day, see Fig. 7. On 26 November 2010, well before the onset of the Geminids, the column density is largest ($2.58 \times 10^{13}\,\mathrm{m}^{-2}$). It decreases over time until 19 December, when the median is $1.81 \times 10^{13}\,\mathrm{m}^{-2}$, the smallest value measured during the period. This means the Na column density decreased by 30 % within 24 days.

Measurements with the Na lidar were also performed in December 2009 and 2011. The times are given in Table 4.

Table 3. Peak density, FWHM of the Na layer, median centroid height, median Na column density and mean temperature at 91 km of both lidar beams for days given in the left column. No FWHM of the Na layer and no temperature were calculated for 5 December and 19 December, respectively.

Date 2010	Peak density	FWHM Na layer	Centroid height	Na column dens.	Mean temperature at 91 km
26 November	$3932 \times 10^6\,m^{-3}$	11.38 km	92.03 km	$2.58 \times 10^{13}\,m^{-2}$	200.8 K
4 December	$3369 \times 10^6\,m^{-3}$	11.45 km	92.95 km	$2.29 \times 10^{13}\,m^{-2}$	199.3 K
5 December	$3258 \times 10^6\,m^{-3}$	–	92.28 km	$2.31 \times 10^{13}\,m^{-2}$	199.2 K
7 December	$3125 \times 10^6\,m^{-3}$	11.65 km	91.45 km	$2.12 \times 10^{13}\,m^{-2}$	198.0 K
13 December	$4493 \times 10^6\,m^{-3}$	7.82 km	91.31 km	$1.95 \times 10^{13}\,m^{-2}$	221.9 K
19 December	$3971 \times 10^6\,m^{-3}$	10.64 km	90.97 km	$1.81 \times 10^{13}\,m^{-2}$	–

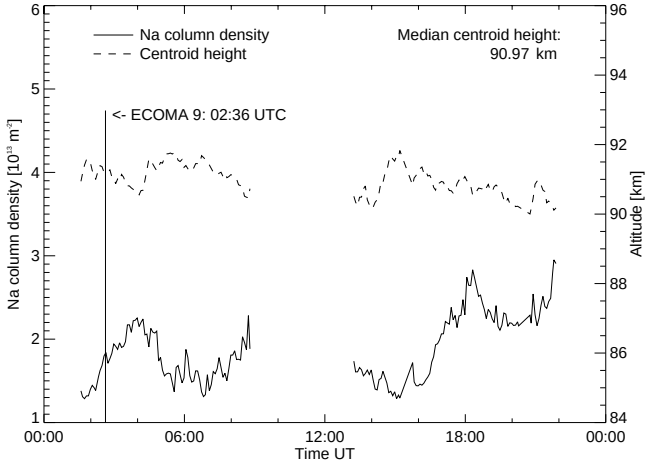

Fig. 5. As Fig. 3, but 19 December 2010. The vertical line indicates the launch of ECOMA 9. The data gap from 08:48 to 13:13 UT is due to daylight conditions.

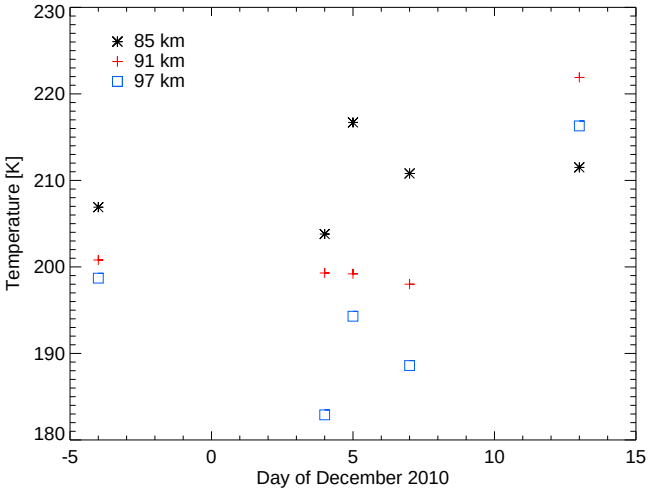

Fig. 6. Time series of temperature at 85 km (black asterisks), 91 km (red plus signs) and 97 km altitude (blue squares) measured with the ALOMAR Na lidar. The temperature values are the mean values of each day from both lidar beams. Dates are given as day of December, i.e. "−4" corresponds to 26 November 2010.

The data from 2009 exhibits an even stronger decrease in Na column density (∼39 %), and on a shorter time scale. While the median column density is largest on 8 December 2009 ($3.52 \times 10^{13}\,m^{-2}$), it decreased within a week to $2.16 \times 10^{13}\,m^{-2}$ on 15 December. There is no measurement data available for 14 December 2009.

In December 2011, we operated the Na lidar on 8, 9, 13 and 16 December. The data show a much larger Na column density than in 2010, but a similar pattern over time. On 8 December 2011, the median column density was $4.34 \times 10^{13}\,m^{-2}$, and $4.09 \times 10^{13}\,m^{-2}$ on 9 December 2011. Near the Geminids maximum (13 December), the median column density decreased to $3.76 \times 10^{13}\,m^{-2}$. It increased to $4.36 \times 10^{13}\,m^{-2}$ on 16 December 2011.

From the three years, ten pairs of consecutive values can be formed. Of these, only three pairs do not show a decrease of median daily Na column density, two show an increase and one shows no change. The day-to-day scatter around a fitted linear trend (not plotted) is definitely smaller than the linear decrease over a week. Only the last pair of values in 2011 does not fit this description. We therefore conclude early December was a period of Na column density decrease in the three years considered.

The mean winter value (i.e. December, January and February) of Na column density in 1985/86 was $5.6 \times 10^{13}\,m^{-2}$ (Tilgner and von Zahn, 1988). This means that our measured values in 2010 correspond to only 32 % to 41 % of that value. In a six-hour Na lidar observation from 10/11 December 1997, which even included a moderate sporadic Na layer, Heinselman et al. (1998) observed column densities of only $1 \times 10^{13}\,m^{-2}$ to $3 \times 10^{13}\,m^{-2}$. Together with our results, this suggests that the Na column density at high latitudes is generally significantly smaller during the Geminids than otherwise in December to February, or at least smaller than in 1985/86. This also means that the year-to-year variability of Na column density is much larger than any effect of the meteor shower.

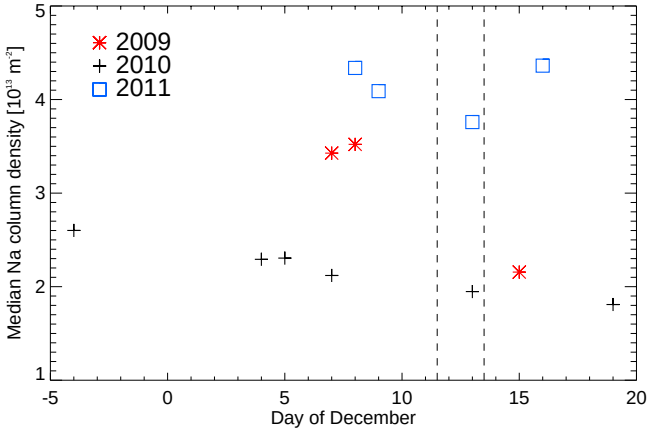

Fig. 7. Time series of daily median value of Na column density (in $10^{13}\,m^{-2}$) as a function of date. Only data for the beam pointed north with a zenith angle of 20° is shown for 2009 (red stars) and 2010 (black plus signs). Data for 2011 (blue squares) is the median of the five-minute averages from both beams pointed to zenith. The measurement uncertainty is two orders of magnitude smaller, and is therefore not plotted. See Figs. 3 to 5 for the geophysical variability. The vertical dashed lines indicate the approximate period of the Geminids peak activity. Dates are given as day of December, i.e. "−4" corresponds to 26 November.

3.3 Correlation of meteors and Na density

The correlation between Na column density and the number of meteors entering Earth's atmosphere is investigated in Fig. 8, covering the time period of the Na lidar measurement on 13 December 2010 from 02:40 UT until 07:20 UT. The left panel shows only meteors that originated from the Geminids radiant, while the right panel shows the number of sporadic meteors. The correlation coefficient is $R = -0.04$ between Na column density and Geminids meteors, and $R = 0.13$ between Na column density and the total number of meteors, that is Geminids plus sporadic meteors (not shown here). Thus, we detect no correlation between Geminids meteors and Na column density.

A very small correlation ($R = 0.25$) exists between the number of sporadic meteors and the Na column density (Fig. 8, right panel).

We caution that such correlations should not be expected, either. By dividing the the column abundance of Na atoms by the estimated meteoric ablation input $4 \times 10^7\,m^{-2}\,s^{-1}$ (Plane, 2004), we obtain an average residence time of a given Na atom of about one week. Therefore, the Na layer integrates variations in the daily input over about one week.

3.4 In situ measurements of meteoric smoke particles

We present in situ data on meteoric smoke particles (MSP) as measured during the three sounding rocket flights on 4, 13, and 19 December 2010 (Fig. 9). For the current purpose we only consider column densities of meteoric smoke particles as derived from the Faraday cup channel data of the ECOMA particle detector (see Sect. 2.3). Details about the determination of these column densities are presented in the companion paper by Rapp et al. (2012). Figure 9 shows that the meteoric smoke particle column density decreased steadily from $5.2 \times 10^{11}\,m^{-2}$ on 4 December, via $4.3 \times 10^{11}\,m^{-2}$ on 13 December to $3.0 \times 10^{11}\,m^{-2}$ on 19 December. We note that this means that there are three independent data sources showing a decrease of meteor related quantities over the considered period of observations. Both the Na column density, the flux of sporadic meteors, as well as the meteoric smoke particle column density all show a steady decrease. We will discuss possible explanations for these observations in Sect. 4.

Table 4. Na lidar measurements in December 2009 and 2011. Only days with more than three hours of data are listed. Times are given in [hh:mm] format in UT. Local time is UT plus one hour.

Day	Na lidar observation
7 December 2009	13:53–22:33
8 December 2009	18:19–23:54
15 December 2009	13:19–16:24
8 December 2011	15:03–23:12
9 December 2011	13:13–21:12
13 December 2011	17:49–22:53
16 December 2011	17:22–20:40

4 Discussion

Since meteors are the source of mesospheric metal species, one could expect their abundance to increase during a major meteor shower like the Geminids. However, our data does not show such an increase. Hake et al. (1972) reported a more than fourfold increase of the Na layer during about four hours on 13/14 December 1971. This may suggest that the Na content of the Geminids varies from year to year, or even has decayed between 1971 and 2010. It cannot be ruled out, though, that something else than the Geminids was the reason for this particular increase.

A decrease in Na abundance of the observed strength in the course of December is not present in previously published observation or model results (Tilgner and von Zahn, 1988; Plane et al., 1999; Gerding et al., 1999).

Our measurements reveal unusually low values of Na column density for wintertime. Temperatures were measured at around 200 K at 91 km altitude, which is typical of the Arctic winter mesopause region. These temperatures cannot explain such a low Na density.

Because the ALOMAR Weber Na lidar was the only metal resonance fluorescence lidar at ALOMAR during the observations reported here, we were not able to measure the ratio of Na to other metallic species from a meteor trail by lidar.

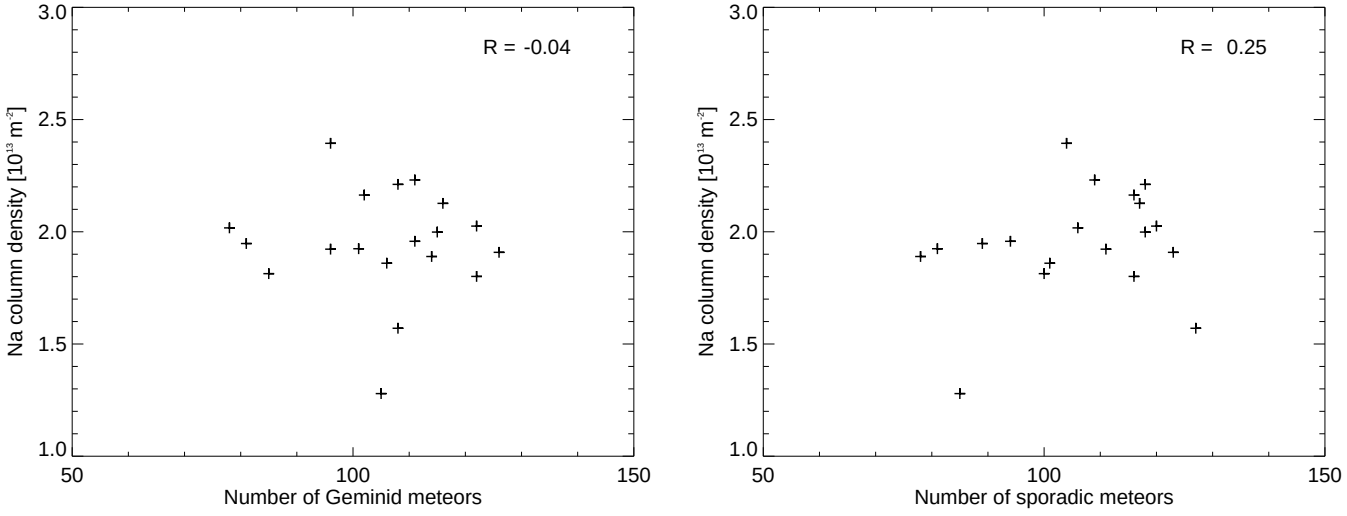

Fig. 8. Scatter plots of Na column density versus Geminids meteor number (left panel) and Na column density versus number of sporadic meteors (right panel) for 13 December 2010, 02:40 to 07:20 UT. Data points are averaged over 15 min. The correlation coefficients (R) are printed in the upper right corner of each panel. The number of Geminids meteors are separated from the sporadic meteors by their radiant of origin.

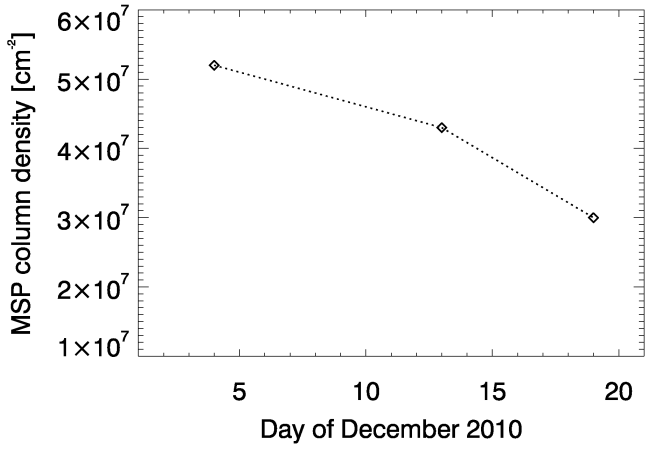

Fig. 9. Column density of meteoric smoke particles (MSP) measured in situ during the launches of ECOMA 7 to 9.

There was no mass spectrometer on board the ECOMA rockets, thus no ion species could be identified.

The inter-annual variation of Na column density appears larger than the variation during the Geminids meteor shower in each of the three years. This seems to indicate that other processes than the Geminids meteor shower play a much greater role for the abundance of Na. These could be chemical processes, transport of constituents, sporadic meteors or a combination of these.

Figure 10 shows a fairly convincing correlation between sporadic meteor echoes (Fig. 7 in Stober et al. (2012), left panel, black line) and Na column density of 2010 from Fig. 7 and that it is in agreement with a correlation between Na abundance and meteoric smoke particles and a correlation between meteoric smoke particles and sporadic meteor echoes.

The factors we have used to normalize the two other datasets to Na column density indicate that there are on average 44 free Na atoms per observed meteoric smoke particle in the upper mesosphere/lower thermosphere. We also get an indication of the number of free Na atoms ablated and the number of meteoric smoke particles generated per sporadic echo observed with the Andenes meteor radar. The latter is, however, dependent on the radar's sensitivity and not purely a geophysical constant.

The error bars show the geophysical variability of Na column density from Figs. 3 to 5. The uncertainty of each datapoint is only approximately 1 % of each value.

With reference to Fig. 7 of Stober et al. (2012), both meteoric smoke particles and Na definitely do not vary as the number of observed Geminid echoes as shown by the red line in their figure. Therefore, our observations are in agreement with an assumption that the Geminids meteor shower contributes very little or nothing to the total number of meteoric smoke particles or to mesospheric Na, but that sporadic meteors definitely do.

These results, and with reference to Stober et al. (2012), suggest that the Geminids do not contribute a relevant fraction to the meteoric mass input. They contain many large, visible meteors, but much fewer small meteors than the sporadic meteor population. We conclude that mainly small meteors ($< 10^{-12}$–10^{-8} kg) are relevant for meteoric smoke particles and for the ablation of Na.

Generally, we can rule out photochemistry as a reason for a decrease in atomic Na because we have only taken data in

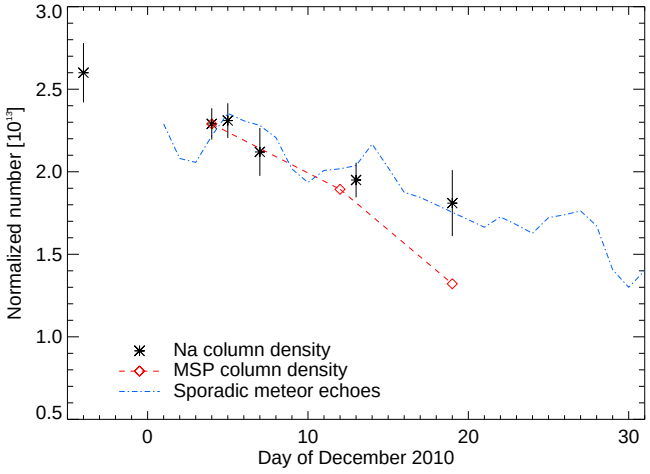

Fig. 10. Comparison of sporadic meteor echoes (blue dash-dot line), Na column density (black asterisks; error bars indicate the standard deviation of the geophysical variability), and MSP column density (red diamonds) in December 2010. The y-axis is correct for Na column density in m^{-2}. The values must be multiplied by 2.27×10^{-2} for absolute MSP column density. The values multiplied by 3.75^{-10} give the correct number of observed sporadic meteor echoes. The number of meteor echoes on 17 to 19 December is interpolated, because the radar was out of order on these days.

darkness, but auroral particle precipitation might be important.

We have checked if a planetary wave may have caused the observed decrease of Na column density. A wavelet analysis of the 2010 Andenes meteor radar wind data showed a planetary wave at 91 and 97 km with an amplitude of $13\,m\,s^{-1}$ and a period of nine days in the meridional direction, and a zonal component with a period of 16 days and an amplitude of 10 to $11\,m\,s^{-1}$. No such wave structure can be seen in our Na lidar data (Figs. 6 and 7).

We have calculated the global total meteoric input per day from two meteor trail observations (Figs. 2a, 2b) during about 40 h of lidar measurements in 2010. The value of $20.2\,t\,d^{-1}$ slightly exceeds the maximum value of $20\,t\,d^{-1}$ given by Plane (2004). For this calculation, we assumed a meteoric composition of ordinary chondrites and that the meteoric input does not vary with latitude. We cannot rule out that the lidar detected more meteors which had a smaller Na density than the background Na density, and were therefore not visible.

5 Conclusions

The Geminids meteor shower did not contribute significantly to the column density of mesospheric Na atoms nor the number of meteoric smoke particles in 2010. We observe a similar tendency in 2009 and 2011. These three years are in contrast to an observation in 1971 by Hake et al. (1972).

The weak decrease of the number of sporadic meteors in 2010 as measured with the meteor radar correlates well with corresponding decreases of Na column density and meteoric smoke particle column density. This correlation suggests that the sum of sporadic meteors contains more material, and more Na, than the sum of Geminids meteors.

We suggest that the Na content of Geminids meteors may vary from year to year, or even has decreased over the last four decades.

We did not happen to observe any sporadic Na layer, but two very short-lived meteor trails at 84 and 87 km. From these two meteor trail observations, we calculated a global meteoric Na flux of $121\,kg\,d^{-1}$ and a global total meteoric influx of $20.2\,t\,d^{-1}$.

The vertical extent of the Na layer was only 7.82 km during the Geminids peak activity, much narrower than usual. The topside reaches the detection limit near 103 km.

We did not observe effects of meteors on the topside, as reported by Höffner and Friedman (2004).

Our measurements reveal unusually low values of Na column density in 2010 for wintertime.

Acknowledgements. The Na lidar work was partially funded by the grant 216870/F50 from the Research Council of Norway. The Norwegian Space Centre and the Research Council of Norway supported the Norwegian contribution to the ECOMA programme with funding through grants 197629 and 191754. T. Dunker and U.-P. Hoppe thank the ALOMAR staff, B. P. Williams and J. Østerpart for their assistance in collecting the data. We thank V. Matthias for the planetary wave analysis.

Topical Editor C. Jacobi thanks B. Clemesha and one anonymous referee for their help in evaluating this paper.

References

Arnold, K. S. and She, C. Y.: Metal fluorescence lidar (light detection and ranging) and the middle atmosphere, Contemp. Phys., 44, 35–49, 2003.

Borovička, J.: Properties of meteoroids from different classes of parent bodies, in: Near Earth objects, our celestial neighbors: opportunity and risk, edited by: Milani, A., Valsecchi, G. B., and Vokrouhlick, D., Proc. Int. Astron. Union, 2, Symposium S236, 107–120, doi:10.1017/S1743921307003134, 2006a.

Borovička, J.: Spectroscopic analysis of Geminids meteoroids, Meteorit. Planet. Sci. Suppl. 41, A25, 2006b.

Bowman, M. R., Gibson, A. J., and Sandford, M. C. W.: Atmospheric sodium measured by a tuned laser radar, Nature, 221, 456–457, 1969.

Chu, X., Pan, W., Papen, G., Gardner, C. S., Swenson, G., and Jenniskens, P.: Characteristics of Fe ablation trails observed during the 1998 Leonids meteor shower, Geophys. Res. Lett., 27, 1807–1810, 2000.

Clemesha, B. R.: Sporadic neutral metal layers in the mesosphere and lower thermosphere, J. Geophys. Res., 57, 725–736, 1995.

Clemesha, B. R., Kirchhoff, V. W. J. H., Simonich, D. M., and Takahashi, H.: Evidence of an extraterrestrial source for the mesospheric sodium layer, Geophys. Res. Lett., 5, 873–876, 1978.

Clemesha, B. R., Simonich, D. M., Batista, P. P., and Kirchhoff, V. W. J. H.: The diurnal variation of atmospheric sodium, J. Geophys. Res., 87, 181–186, 1982.

Clemesha, B. R., Batista, P. P., and Simonich, D. M.: An evaluation of the evidence for ion recombination as a source of sporadic neutral layers in the lower thermosphere, Adv. Space Res., 24, 547–556, 1999.

Correira, J., Aikin, A. C., Grebowsky, J. M., and Burrows, J. P.: Metal concentrations in the upper atmosphere during meteor showers, Atmos. Chem. Phys., 10, 909–917, doi:10.5194/acp-10-909-2010, 2010.

Cox, R. M. and Plane, J. M. C.: An ion-molecule mechanism for the formation of neutral sporadic Na layers, J. Geophys. Res., 103, 6349–6359, 1998.

Fricke, K. H. and von Zahn, U.: Mesopause temperatures derived from probing the hyperfine structure of the D_2 resonance line of sodium by lidar, J. Atmos. Terr. Phys., 47, 499–512, 1985.

Gardner, C. S., Voelz, D. G., Sechrist, Jr., C. F., and Segal, A. C.: Lidar studies of the nighttime sodium layer over Urbana, Illinois: 1. Seasonal and nocturnal variations, J. Geophys. Res., 91, 13659–13674, 1986.

Gerding, M., Alpers, M., Höffner, J., and von Zahn, U.: Simultaneous K and Ca lidar observations during a meteor shower on March 6/7, 1997, at Kühlungsborn, Germany, J. Geophys. Res., 104, 24689–24698, 1999.

Gibson, A. J., Thomas, L., and Bhattacharyya, S. K.: Laser observations of the ground-state hyperfine structure of sodium and of temperatures in the upper atmosphere, Nature, 281, 131–132, doi:10.1038/281131a0, 1979.

Granier, C. and Mégie, G.: Daytime lidar measurements of the mesospheric sodium layer, Planet. Space Sci., 30, 169–177, 1982.

Hake, R. D., Arnold, D. E., Jackson, D. W., Evans, W. E., Ficklin, B. P., and Long, R. A.: Dye-laser observations of the nighttime atomic sodium layer, J. Geophys. Res., 77, 6839–6848, 1972.

Hansen, G. and von Zahn, U.: Sudden sodium layers in polar latitudes, J. Atmos. Terr. Phys., 52, 585–608, 1990.

Havnes, O., Trøim, J., Blix, T., Mortensen, W., Næsheim, L. I., Thrane, E., and Tønnesen, T.: First detection of charged dust particles in Earth's mesosphere, J. Geophys. Res., 101, 10839–10847, doi:10.1029/96JA00003, 1996.

Heinrich, D.: Temperature and sodium density studies in the Arctic mesopause region based on measurements with the ALOMAR Weber sodium lidar, Ph.D. thesis, University of Oslo, Norway, 2007.

Heinrich, D., Nesse, H., Blum, U., Acott, P., Williams, B., and Hoppe, U.-P.: Summer sudden Na number density enhancements measured with the ALOMAR Weber Na Lidar, Ann. Geophys., 26, 1057–1069, doi:10.5194/angeo-26-1057-2008, 2008.

Heinselman, C. J.: Auroral effects on the gas phase chemistry of meteoric sodium, J. Geophys. Res., 105, 12181–12192, 2000.

Heinselman, C. J., Thayer, J. P., and Watkins, B. J.: A high-latitude observation of sporadic sodium and sporadic E-layer formation, Geophys. Res. Lett., 25, 2059–3062, 1998.

Helmer, M. and Plane, J. M. C.: A study of the reaction NaO_2 + O $\rightarrow$ NaO + O_2: implications for the chemistry of sodium in the upper atmosphere, J. Geophys. Res., 98, 23207–23222, 1993.

Höffner, J. and Friedman, J. S.: The mesospheric metal layer topside: a possible connection to meteoroids, Atmos. Chem. Phys., 4, 801–808, doi:10.5194/acp-4-801-2004, 2004.

Höffner, J., von Zahn, U., McNeil, W. J., and Murad, E.: The 1996 Leonid shower as studied with a potassium lidar: observations and inferred meteoroid sizes, J. Geophys. Res., 104, 2633–2643, 1999.

Höffner, J., Fricke-Begemann, C., and von Zahn, U.: Note on the reaction of the upper atmosphere potassium layer to the 1999 Leonid meteor storm, Earth Moon Planets, 82–83, 555–564, 2000.

Hughes, D. W.: Meteors, in: Cosmic dust, edited by: McDonnell, J. A. M., John Wiley & Sons, Chichester, 123–185, 1978.

Junge, C. E., Oldenberg, O., and Wasson, J. T.: On the origin of the sodium present in the upper atmosphere, J. Geophys. Res., 67, 1027–1039, 1962.

Kaifler, B.: Na lidar at ALOMAR – electrooptic improvements, analysis algorithms and selected atmospheric observations 80 to 100 km above northern Norway, Diploma thesis, Ulm University, Germany, 2009.

Kalashnikova, O., Horanyi, M., Thomas, G. E., and Toon, O. B.: Meteoric smoke production in the atmosphere, Geophys. Res. Lett., 27, 3293–3296, 2000.

Kopp, E.: On the abundance of metal ions in the lower ionosphere, J. Geophys. Res., 102, 9667–9674, 1997.

Lübken, F.-J. and von Zahn, U.: Thermal structure of the mesopause region at polar latitudes, J. Geophys. Res., 96, 20841–20857, 1991.

Mason, B.: Handbook of elemental abundances of the elements in meteorites, Gordon and Breach, Newark, NJ, USA, 1971.

McNeil, W. J., Murad, E., and Lai, S. T.: Comprehensive model for the atmospheric sodium layer, J. Geophys. Res., 100, 16847–16855, 1995.

Nesse, H., Heinrich, D., Williams, B., Hoppe, U.-P., Stadsnes, J., Rietveld, M., Singer, W., Blum, U., Sandanger, M. I., and Trondsen, E.: A case study of a sporadic sodium layer observed by the ALOMAR Weber Na lidar, Ann. Geophys., 26, 1071–1081, doi:10.5194/angeo-26-1071-2008, 2008.

Neuber, R., von der Gathen, P., and von Zahn, U.: Altitude and temperature of the mesopause at 69° N latitude in winter, J. Geophys. Res., 93, 11093–11101, 1988.

Plane, J. M. C.: The role of sodium bicarbonate in the nucleation of noctilucent clouds, Ann. Geophys., 18, 807–814, doi:10.1007/s00585-000-0807-2, 2000.

Plane, J. M. C.: Atmospheric chemistry of meteoric metals, Chem. Rev., 103, 4963–4984, 2003.

Plane, J. M. C.: A time-resolved model of the mesospheric Na layer: constraints on the meteor input function, Atmos. Chem. Phys., 4, 627–638, doi:10.5194/acp-4-627-2004, 2004.

Plane, J. M. C., Cox, R., Qian, J., Pfenninger, W. M., Papen, G. C., Gardner, C. S., and Espy, P. J.: Mesospheric Na layer at extreme high latitudes in summer, J. Geophys. Res., 103, 6381–6389, 1998.

Plane, J. M. C., Gardner, C. S., Yu, J., She, C. Y., Garcia, R. R., and Pumphrey, H. C.: Mesospheric Na layer at 40° N: modeling and observations, J. Geophys. Res., 104, 3773–3788, 1999.

Rapp, M. and Strelnikova, I.: Measurements of meteor smoke particles during the ECOMA–2006 campaign: 1. particle detection by

active photoionization, J. Atmos. Sol.-Terr. Phys., 71, 477–485, doi:10.1016/j.jastp.2008.06.002, 2009.

Rapp, M., Strelnikova, I., Strelnikov, B., Hoffmann, P., Friedrich, M., Gumbel, J., Megner, L., Hoppe, U.-P., Robertson, S., Knappmiller, S., Wolff, M., and Marsh, D., R.: Rocket-borne in situ measurements of meteor smoke: Charging poperties and implications for seasonal variation, J. Geophys. Res., 115, D00I16, doi:10.1029/2009JD012725, 2010.

Rapp, M., Plane, J. M. C., Strelnikov, B., Stober, G., Ernst, S., Hedin, J., Friedrich, M., and Hoppe, U.-P.: In situ observations of meteor smoke particles (MSP) during the Geminids 2010: constraints on MSP size, work function and composition, Ann. Geophys., 30, 1661–1673, doi:10.5194/angeo-30-1661-2012, 2012.

Rietmeijer, F. J. M.: Mesospheric metal abundances and meteoric dust: analyses of surviving meteoroids, Adv. Space Res., 33, 1475–1480, 2003.

She, C. Y., Williams, B. P., Hoffmann, P., Latteck, R., Baumgarten, G., Vance, J. D., Fiedler, J., Acott, P., Fritts, D. C., and Lübken, F. J.: Simultaneous observations of sodium atoms, NLC and PMSE in the summer mesopause region above ALOMAR, Norway (69.3° N, 12° E), J. Atmos. Sol.-Terr. Phys., 68, 93–101, 2002.

Singer, W., von Zahn, U., and Weiß, J.: Diurnal and annual variations of meteor rates at the arctic circle, Atmos. Chem. Phys., 4, 1355–1363, doi:10.5194/acp-4-1355-2004, 2004.

Slipher, V. M.: Emissions in the spectrum of the light of the night sky, Publ. Astron. Soc. Pac., 41, 262–263, 1929.

Stober, G., Schult, C., Baumann, C., Latteck, R., and Rapp, M.: The Geminid Meteor Shower during the ECOMA Sounding Rocket Campaign: specular and head echo radar observations, Ann. Geophys., in review, 2012.

Szewczyk, A., Strelnikov, B., Rapp, M., Strelnikova, I., Baumgarten, G., Kaifler, N., Dunker, T., and Hoppe, U.-P.: Simultaneous observations of a Mesospheric Inversion Layer and turbulence during the ECOMA-2010 rocket campaign, Ann. Geophys., in review, 2012.

Tilgner, C. and von Zahn, U.: Average properties of the sodium density distribution as observed at 69° N latitude in winter, J. Geophys. Res., 93, 8439–8454, 1988.

Thomas, L. and Bhattacharyya, S. K.: Mesospheric temperatures deduced from laser observations of the Na D_2 line profile, ESA SP152, 49–50, 1980.

Uchiumi, M., Nagasawa, C., Hirono, M., Fujiwara, M., and Maeda, M.: Sporadic enhancement of the mesospheric sodium during the Perseids γ meteor shower, J. Geomag. Geoelectr., 45, 393–402, 1993.

von Zahn, U. and Hansen, T. L.: Sudden neutral sodium layers: A strong link to sporadic E, J. Atmos. Terr. Phys., 50, 93–104, 1988.

von Zahn, U., von der Gathen, P., and Hansen, G.: Forced release of sodium from upper atmospheric dust particles, Geophys. Res. Lett., 14, 76–79, 1987.

von Zahn, U., von Cossart, G., Fiedler, J., Fricke, K. H., Nelke, G., Baumgarten, G., Rees, D., Hauchecorne, A., and Adolfsen, K.: The ALOMAR Rayleigh/Mie/Raman lidar: objectives, configuration, and performance, Ann. Geophys., 18, 815–833, doi:10.1007/s00585-000-0815-2, 2000.